Ion pairing effects in intramolecular heterolytic H_2 activation in an Ir(III) complex: a combined theoretical/experimental study

Karin Gruet,[a] Eric Clot,*[b] Odile Eisenstein,*[b] Dong Heon Lee,[ad] Ben Patel,[a] Alceo Macchioni*[c] and Robert H. Crabtree*[a]

[a] *Department of Chemistry, Yale University, New Haven, CT 06520-8107, USA. E-mail: robert.crabtree@yale.edu*
[b] *LSDSMS (UMR 5636), Case courrier 14, Université Montpellier 2, 34095, Montpellier cedex 5, France. E-mail: odile.eisenstein@univ-montp2.frclot@univ-montp2.fr*
[c] *Dipartimento di Chimica, Università di Perugia, Via Elce di Sotto 8, 06123, Perugia, Italy. E-mail: alceo@unipg.it*
[d] *Department of Chemistry, Chonbuk National University, Chonju 561-756, Korea*

Received (in Montpellier, France) 25th July 2002, Accepted 10th September 2002
First published as an Advance Article on the web 31st October 2002

A free pendant 2-amino group in a benzoquinolinate ligand bound to Ir(III) can cause heterolytic dissociation of an adjacent Ir–H_2, depending on the nature of the phosphine, L. For L = $PMePh_2$, heterolysis does not occur and an H_2 complex, $[IrH(H_2)(bq\text{-}NH_2)L_2]BF_4$, is seen, but if L = PPh_3 or PCy_3, heterolysis does occur and a hydride product, $[IrH_2(bq\text{-}NH_3)L_2]BF_4$, is formed by proton transfer from the bound H_2 to the pendant NH_2 group. The electronic effect of L is not dominant. Theoretical studies (DFT calculations) show that the H_2 complex is predicted to be more stable for all the phosphines used, if the anion is ignored. We propose that the hydride isomer, formed when L is bulky, depends on ion pairing effects for its stability. The calculated electrostatic potentials for the two isomers suggest that the counter anion has to be located much closer to the metal in the H_2 complex than in the hydride where the anion is much farther from the metal. The bulky phosphines PPh_3 and PCy_3 favor remote ion pairing and therefore favor the hydride isomer because steric effects disfavor close ion pairing as confirmed by ONIOM (B3PW91/UFF) calculations of the ion pair geometry. An improved synthesis of $[IrH_5(PCy_3)_2]$ is reported.

Introduction

Heterolytic H_2 activation[1] (eqn. 1), currently attracting increasing attention, may often go *via* an acidic H_2 complex.[2] For example, an all-Fe hydrogenase has recently been proposed to contain a basic amino group immediately adjacent to the H_2 binding site capable of acting as a base for deprotonating coordinated H_2.[3]

$$L_nM^+ \xrightarrow{H_2} L_nM(H_2)^+ \xrightarrow{B} L_nM\text{-}H + BH^+ \quad (1)$$
(B = base; L_n = ligands)

We have briefly reported[4] on a 2-aminobenzoquinolinate ($bq\text{-}NH_2$) Ir(III) complex, designed to favor heterolysis of H_2. The free $-NH_2$, located on the bq framework near the H_2 binding site, can act as an intramolecular base causing proton abstraction from H_2. The rigidity of the bq framework prevents the amino group from directly binding to the metal, which would block the H_2 binding site. Broadly similar complexes with an H_2 binding site and a basic group on a ligand have been reported by Morris, Sabo-Etienne and Chaudret.[5,6] We reported[4] that moving from PPh_3 to more basic ligands such as $PMePh_2$ led to the formation of an H_2 complex without heterolysis, so we ascribed the difference to an electronic effect. The work described here shows that this proposal is invalid since the very basic PCy_3 also gives heterolysis. We have now looked for the origin of this effect by a combined experimental/theoretical study on this system. This leads us to propose that ion pairing is the key factor that favors heterolysis for bulky phosphines because the anion binding site for the hydride heterolysis product is more remote from the metal. Ion pairing has been implicated in a few other organometallic systems.[7]

Results and discussion

Choice of system

In order to separate out the effect of the pendant amino group, we needed to compare the 2-aminobenzoquinolinate ($bq\text{-}NH_2$) system with the benzoquinolinate system, studied previously,[8] lacking a pendant amino group (bq-H). In this early work with bq-H (eqn. 2), we showed that H_2 replaces a labile ligand such as water or acetone in the starting material, **1**, to give the H_2 complex, **2**. Bases such as excess NEt_3 cause deprotonation and H_2 heterolysis to give the hydride, **3**.

In the prior communication[4] we reported that, depending on the phosphine, the aqua complex $[IrH(bq\text{-}NH_2)(OH_2)(L)_2]BF_4$, **4**, reacts with H_2 to afford either the dihydrogen compound $[IrH(H_2)(bq\text{-}NH_2)(L)_2]BF_4$, **5**, or the hydride $[IrH_2(bq\text{-}NH_3)(L)_2]BF_4$, **6** (eqn. 3). Only dihydrogen compounds **5** were obtained upon hydrogenation of the parent system $[IrH(bq\text{-}H)(OH_2)(PPh_3)_2]BF_4$, **1**, bearing no adjacent pendant group.[8] Since the dihydrogen compounds of type **5** were originally[4] obtained only with the more basic alkyl phosphines and the hydride **6** with the less basic PPh_3, we ascribed this behavior to the electronic effect of the phosphines. We now report the hydride **6** also forms with the very basic PCy_3 which has now led us to carry out a combined theoretical/experimental study that identifies a steric effect acting in the

 DOI: 10.1039/b207339k

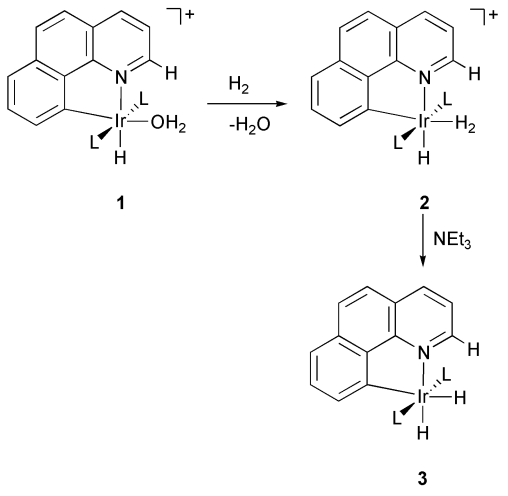

1 2 3 (2)

alternate ion pairs formed from **5** and **6** as the proposed origin of the effect.

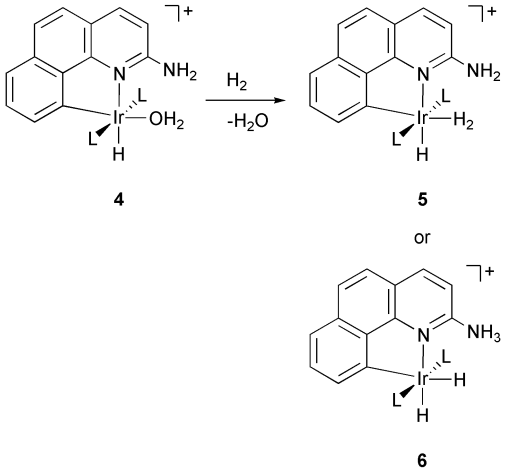

4 5 6 (3)

Synthesis

The required ligand precursor, 2-amino-7,8-benzoquinoline, was readily prepared from 7,8-benzoquinoline and $NaNH_2$.[9,10] Most of the required starting aqua complexes $[IrH(bq\text{-}NH_2)(OH_2)L_2]BF_4$ (**4**: **a**, L = PPh_3; **b**, L = P(*p*-$C_6H_4CH_3)_3$; **c**, L = P(*p*-$C_6H_4OCH_3)_3$; **d**, L = $PMePh_2$) are known (**4a**)[10] or could be synthesized by the known route[10] or variants described in the experimental section. All were fully characterized as detailed in the experimental section or in prior papers. These syntheses (Scheme 1) involve cyclometalation of 2-aminobenzoquinoline with $[(cod)IrL_2]X/H_2$[10] or using preformed $[IrH_2(OH_2)_2L_2]X$ in moist CH_2Cl_2 at room temperature to give the aqua complex $[IrH(bq\text{-}NH_2)(OH_2)L_2]X$ (**4**, bq-NH_2 = 2-benzoquinolinato; X = BF_4 or PF_6) or using preformed $[IrH_2(Me_2CO)_2L_2]X$ in acetone at room temperature to give the acetone complex $[IrH(bq\text{-}NH_2)(Me_2CO)L_2]BF_4$ (**4′**, the prime means acetone is the labile ligand).

The required PCy_3 acetone complex $[IrH(bq\text{-}NH_2)(OCMe_2)(PCy_3)_2]BF_4$ (**4′e**) had not previously been reported and some synthetic effort proved to be necessary to obtain it because the standard route[10] from $[(cod)Ir(PR_3)_2]BF_4/H_2$, used above, was not available as $[(cod)Ir(PCy_3)_2]X$ is unknown. Instead we have prepared it from the known[11] $[IrH_5(PCy_3)_2]$ by protonation in acetone with HBF_4 to give $[Ir(PCy_3)_2(OCMe_2)_2(H)_2]BF_4$ *in situ*, followed by reaction with 2-aminobenzoquinoline to give the desired **4′e**. Surprisingly, it was not possible to synthesize the aqua species for L = PCy_3 but the acetone complex proved well behaved. Otherwise, the results were not dependent on the nature of the leaving group, acetone or water, or on the nature of the anion, BF_4^- or PF_6^-.

We also report an improved synthesis of $[IrH_5(PCy_3)_2]$ by a one step route from commercial $[Ir(cod)Cl]_2$, treatment of which in CH_2Cl_2 with NaOMe and PCy_3 under H_2 gives the product in 59% yield. The isolation of the analytically pure pentahydride only requires filtration and washing. The spectroscopic characterization, ^1H NMR: −11.27 ppm (t, $^2J_{HP}$ = 12.21 Hz), ^{31}P NMR: 33.42 ppm (s), IR: ν(Ir–H) = 1929.1 cm^{-1}, is in full agreement with the published data.[11]

Reaction of 4a–d with H_2: experiment

At −70 °C in CD_2Cl_2, the aqua complex, $[IrH(bq\text{-}NH_2)(OH_2)(PPh_3)_2]BF_4$, **4a**, reacts with H_2 to give the hydride, $[IrH_2(bq\text{-}NH_3)(PPh_3)_2]BF_4$, **6a**, *via* H_2 heterolysis. The ^1H NMR spectrum shows two sharp hydride resonances in the terminal Ir–H region at −23.24 ppm and −25.63 ppm that are coupled to the *cis*-phosphines and to each other (dt, $^2J_{HH'}$ = 8.50 Hz; $^2J_{PH}$ = 14.65 Hz). These are clearly normal

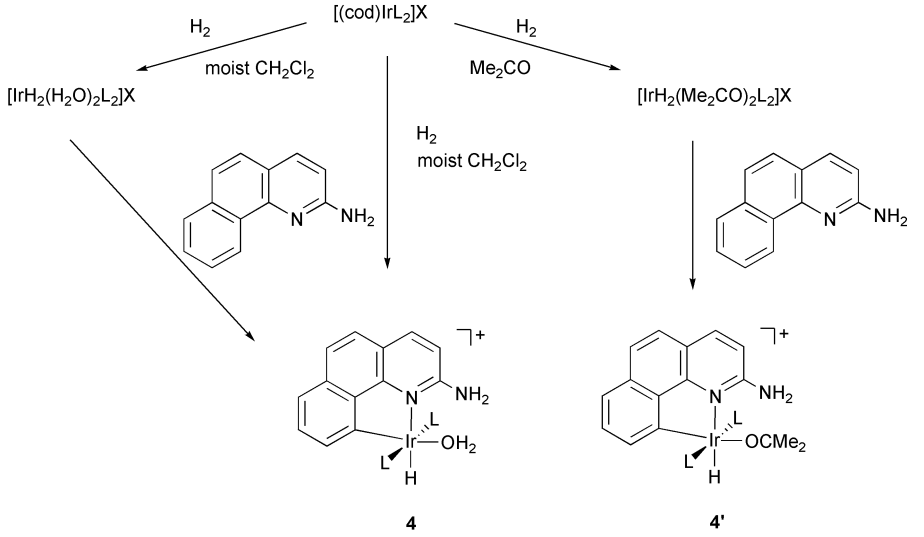

4 4′

(L = PPh_3, **a**; P(p-tolyl)$_3$, **b**; P(p-$MeOC_6H_4)_3$, **c**; $PMePh_2$, **d**; PCy_3, **e**; X = BF_4 or PF_6; cod = 1,5-cyclooctadiene

Scheme 1

hydrides with the normal $^2J_{HH'}$ and $^2J_{PH}$ values usually seen[10] in these systems. A broad resonance at 4.56 ppm of intensity 3H is assigned to the bq-NH_3^+ protons for compound **6a**. The triplet hydride resonance at −16.22 ppm ($^2J_{PH}$ = 14.65 Hz) and the amino resonance at 6.23 ppm characteristic of the starting material **4a** reappears on passing a stream of N_2, showing this conversion is reversible. The presence of anhydrous $MgSO_4$ in the NMR tube is helpful to remove water and drive the equilibrium over to **6.**

In an effort to see if an electronic effect operates in the PAr_3 system, we looked at the phosphines, P(*p*-$C_6H_4CH_3)_3$ and P(*p*-$C_6H_4OCH_3)_3$. Hydride complexes were also obtained both with P(*p*-$C_6H_4CH_3)_3$, **6b**, and P(*p*-$C_6H_4OCH_3)_3$, **6c**. Warming the samples to room temperature led to loss of H_2 below −20 °C, with regeneration of the starting aqua complex, so none of **6a–c** could be isolated as solids.

Changing the phosphine to $PMePh_2$ gave a very different result. The appropriate aqua complex, $[IrH(bq\text{-}NH_2)(OH_2)(PMePh_2)_2]BF_4$, **4d**, also reacts with H_2 at −70 °C but to give the H_2 complex $[IrH(H_2)(bq\text{-}NH_2)(PMePh_2)_2]BF_4$, **5d**. This assignment follows from the very different ^{1}H NMR spectrum. The NH_2 and hydride peaks characteristic of compound **4d** disappear and are replaced by three new signals: an Ir–H triplet at −15.90 ppm ($^2J_{PH}$ = 14.65 Hz) of intensity 1H, a characteristic broad Ir(H_2) resonance of intensity 2H at −3.75 ppm, and a broad NH_2 resonance of intensity 2H at 6.15 ppm appropriate for compound **5d**. As noted previously, an H_2 complex was also seen with PEt_2Ph and P(*n*-Bu)$_3$, but we report only the $PMePh_2$ case in full here because unlike the oily PEt_2Ph and P(*n*-Bu)$_3$ species, complex **4d** crystallized well and its characterization was completely convincing. Like **6**, **5** also loses H_2 on warming above −20 °C, and so cannot be isolated as a solid.

The nature of the leaving group was not important: upon exposure to hydrogen, the acetone complexes (**4′a–d**) also afford the same compounds, H_2 complex **5** or hydride **6**, with exactly the same dependence on the phosphines as is obtained from the analogous aqua complex. However, the hydrogenation is complete only for **4′a** and **4′e**, not for **4′b–d**, no doubt because the acetone is slightly more strongly bound than water.

An electronic effect?

Because less basic phosphines led to the hydride complexes, whereas more basic phosphines led to the dihydrogen complexes, we proposed in the prior communication[4] that the change in the heterolytic H_2 activation equilibrium was due to the electronic effects of the phosphines. We expected the basicity of the phosphine to influence the pK_a of coordinated H_2. In free H_2, the pK_a is *ca.* 35, but upon binding to the metal, it becomes very much more acidic (15 to −5).[5,6] This acidification may be due to the metal fragment stabilizing the H^- product of the heterolytic dissociation while binding H_2 relatively weakly. A basic phosphine should enhance the back bonding to the empty σ* orbital of H_2, causing tighter H_2 binding and lowered acidity. To check this electronic interpretation, we decided to examine the case of PCy_3, the most basic, but also one of the most bulky phosphines in common use. If electronic factors dominate, an H_2 complex should be formed.

Reaction of the PCy_3 complex, 4′e, with H_2: experiment

In complete disaccord with the electronic effect model, hydrogenation of the PCy_3 acetone complex **4′e**, at −80 °C in CD_2Cl_2, led to the hydride compound **6e** with heterolytic H_2 activation. This follows from the disappearance of the triplet Ir–H signal at −14.23 ppm ($^2J_{HP}$ = 14.65 Hz, 1H), and of the broad NH_2 signal at 5.83 ppm (2H) of the amino group, with the appearance of two broad signals for the *cis*-hydrides at −25.06 (1H) and −21.04 ppm (1H), as well as a broad signal at 4.29 ppm (3H) assigned to the ammonium protons. Had the electronic effect been dominant, the basic PCy_3 ligand should have afforded the H_2 complex, but NMR resonances for this species were completely absent and the spectra of the two forms are so different that no doubt is possible.

To eliminate the very remote possibility that the ligands L in this series do not exert their usual electronic effects, we made the carbonyl derivatives of **4a–d** and **4′e** by reaction with CO at 1 atm in CH_2Cl_2 (eqn. 4). As expected, these showed *ν*(CO) IR frequencies entirely consistent with the usual increasing Tolman[12] basicity order (values in parentheses): PPh_3, 2026 (2068.9); P(*p*-$C_6H_4CH_3)_3$, 2024 (2066.7); P(*p*-$C_6H_4OCH_3)_3$, 2023 (2066.1); $PMePh_2$, 2021 (2067.0); PCy_3, 1995 (2056.4) cm^{-1}. Our system is more sensitive to variation in the phosphine than is Tolman's classic $LNi(CO)_3$, because we have a PR_3/CO ratio of 2:1 *versus* 1:3 for Tolman. The increase in basicity on moving to PCy_3 was very large, as expected, and so we can rule out an unexpected inversion of basicity in this case.

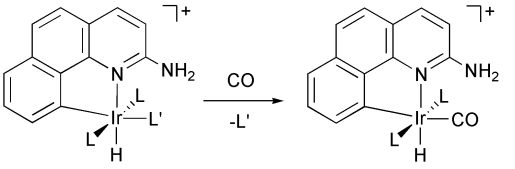

(L' = H_2O or Me_2CO) (4)

4

Initial theoretical analysis

The first model systems studied (DFT, B3PW91)[13] were dihydrogen complex $[Ir(bq\text{-}NH_2)(PH_3)_2(H_2)(H)]^+$ (**7**) and hydride $[Ir(bq\text{-}NH_3)(PH_3)_2(H)_2]^+$ (**8**), where the only differences *versus* the experimental compounds **5** and **6** are the phosphine ligand (PH_3 *vs.* PPh_3) and the absence of anion. The optimized geometries are shown in Fig. 1 and selected geometrical parameters are given in Table 1. The key finding is that dihydrogen complex **7** is strongly favored theoretically with a convincingly large energy preference of 14.4 kcal mol^{-1} while the hydride **6** (L = PPh_3) is favored experimentally. The H–H distance of the dihydrogen complex, 0.87 Å, is normal. Also notable is the dihydrogen bonded[14] N–H···H–Ir group of the hydride form **8** with its short H···H distance of 1.379 Å.

A problem with **7** and **8** is the use of PH_3 as model ligand, since this is neither electronically or sterically comparable with the experimental ligands. To probe the electronic issue, we calculated the situation for the series $PH_{3-x}F_x$ (x = 0–3) to look at the sensitivity of the equilibrium **7**/**8** as a function of change of the phosphine electronic effect. The Tolman[12] electronic parameters (TEPs) for these ligands are: PH_3, 2083.2; PH_2F, 2090.9; PHF_2, 2100.9; PF_3, 2110.8 cm^{-1}, so they cover a broad range of values going from the range typical for

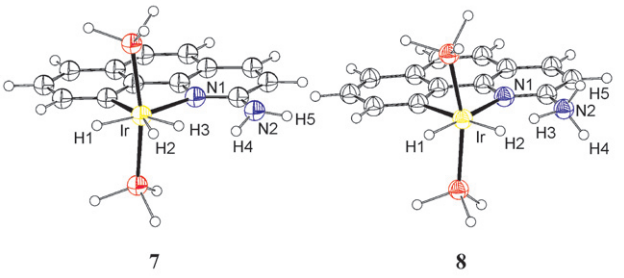

7 **8**

Fig. 1 Optimized geometry (B3PW91) for the dihydrogen complex $IrH(H_2)(bq\text{-}NH_2)(PH_3)_2^+$, **7**, and the hydride complex $Ir(H)_2(bq\text{-}NH_3)(PH_3)_2^+$, **8**.

Table 1 Geometrical parameters (distances in Å, angles in degrees) for the dihydrogen complexes $IrH(H_2)(bq\text{-}NH_2)(PH_xF_{3-x})_2^+$, **7**, and the hydride complexes $Ir(H)_2(bq\text{-}NH_3)(PH_xF_{3-x})_2^+$, **8**, for $x = 0$–3. The relative electronic energy (ΔE/kcal mol^{-1}) and relative free enthalpy (ΔG/kcal mol^{-1}) correspond to the transformation **8** → **7**. The numbering of the hydrogen atoms is shown in Fig. 1 for the PH_3 case

		PH_3	PH_2F	PHF_2	PF_3
Complex **7**	H2–H3	0.870	0.866	0.858	0.850
	H3···H4	1.912	1.963	2.055	2.126
	N2–H4	1.008	1.009	1.010	1.012
Complex **8**	Ir–H2	1.698	1.674	1.673	1.682
	H2···H3	1.379	1.479	1.494	1.613
	N2–H3	1.150	1.111	1.095	1.074
	∠Ir–H2···H3	94.2	94.7	97.0	95.7
	∠H2···H3–N2	176.5	178.7	178.5	176.9
8 → **7**	ΔE	−14.4	−6.6	−2.1	+1.0
	ΔG	−15.6	−9.4	−4.0	+0.8

phosphites to that of CO.[15] PH_3 is a significantly less strong donor than PPh_3 or $P(alkyl)_3$, however, so we felt the need to look at the trend for $PH_{3-x}F_x$ and extrapolate it into a region more appropriate to the experimental phosphines. The resulting trend in calculated ΔG for **7**/**8**, plotted against the TEP (Fig. 2), shows that the dihydrogen complex **7** is still favored for all L more basic than PHF_2; only for the extremely electron-withdrawing ligand PF_3, does the system favor hydride **8**. This implies that within the assumptions made in the calculation, the experimental systems would have been expected to strongly favor the dihydrogen complex **7** for all the experimental phosphines, since these are all much more strongly electron-donating than PHF_2.

Dihydrogen bonding

Also of interest in these calculations is the change of the N–H and H···H bond lengths as the phosphine is varied (Table 1). This indicates that the dihydrogen bonding[14] is strongly enhanced by the more donor ligands. Increasing donor power of the phosphine is expected to enhance the basic character of the metal–hydride bond and therefore enhance dihydrogen bonding. As shown in Fig. 3, the N–H bond elongates significantly and the H···H distance dramatically shortens on moving to more donor phosphines. The H···H distance of 1.379 Å for PH_3 is far shorter than any experimentally observed value; these are usually[14] in the range 1.7–2.0 Å.

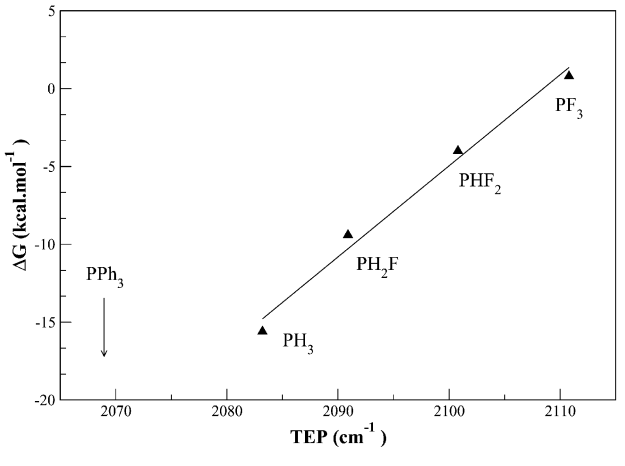

Fig. 2 Evolution of the free enthalpy ΔG (kcal mol^{-1}) for the transformation **8** → **7** as a function of the Tolman Electronic Parameter (TEP)[12,15] for the different PH_xF_{3-x} considered.

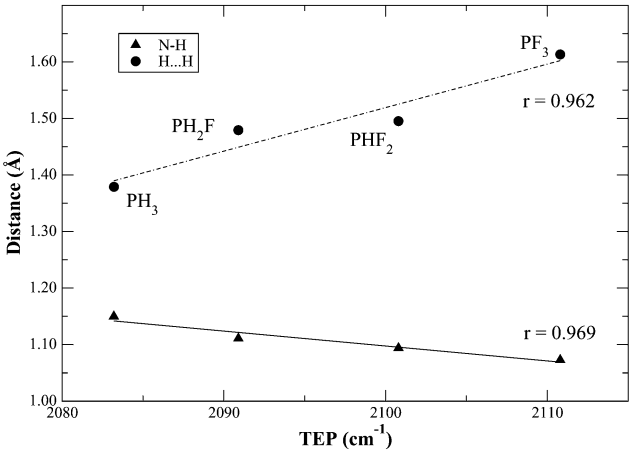

Fig. 3 Change in the H2···H3 and N2–H3 bond distances (Å) in **8** as a function of TEP[12,15] for the different PH_xF_{3-x} considered. See Fig. 1 for the atom numbering in **8**.

Ion pairing effects

The theoretical analysis above indicates that all the phosphines in the series chosen would be expected to give the dihydrogen form and heterolysis should never be observed except with ligands like PF_3 that are far less donating than any used experimentally. In searching for possible explanations, we noted that both of the anomalous cases where heterolysis was observed involve bulky (PPh_3) or very bulky (PCy_3) phosphines. It seemed very unlikely that this bulk could have a direct influence on the $M(H_2)(bq\text{-}NH_2)/MH(bq\text{-}NH_3)$ interconversion because both H_2 and H ligands are sterically small and the energy deficit to be compensated is so large.

Large energies are known to arise by ion pairing: in CH_2Cl_2; these are typically in the range of 20–30 kcal mol^{-1} for organic cases.[16] Very similar complexes to the present ones such as $[Ir(PRPh_2)_2(dipy)(H)_2]X$ (R = Ph, Me, X = BF_4, PF_6, CF_3SO_3, BPh_4) have been unambiguously shown in our prior NMR work to give rise to tight ion pairing in CH_2Cl_2.[17] In these stable complexes, the location of the anion, identified by NOE studies, was near the dipy ligand, on the side remote from the metal. Our prior theoretical analysis[17] using the calculated electrostatic potential of the molecule reproduced the experimental location of the counterion, lending credence to this approach. The present bq system, with its extra benzene ring in the heterocyclic ligand blocking the binding site found for the dipy complex, is expected to strongly disfavor such binding. Instead, we thought ion pairing might occur near the H_2 of the H_2 complex and the $bq\text{-}NH_3$ group of the hydride complex. In this case, the electronically expected H_2 isomer could only be favored in practice if the ion pairing could occur unhindered by bulky L. If L is bulky, we thought that remote ion pairing at the $bq\text{-}NH_3$ site might be the only allowed configuration thus favoring the hydride isomer.

The calculated electrostatic potential contour plots in the bq plane of the two isomers are very different, consistent with our picture of ion pairing at close *versus* remote sites. Fig. 4 illustrates the situation. The $M(H_2)(bq\text{-}NH_2)$ isomer has a preferred anion binding region between the (H_2) ligand and the ($-NH_2$) group, close to the metal. In contrast, the MH($bq\text{-}NH_3$) isomer strongly prefers anion binding in the vicinity of the ($-NH_3$) group, far from the metal (Scheme 2). This difference may be the factor that for bulky L favors the MH($bq\text{-}NH_3$) isomer, with its remote anion binding site, over the $M(H_2)(bq\text{-}NH_2)$ isomer, with its anion binding site close to the metal and also to the bulky PR_3 ligands.

To confirm this analysis, combined quantum mechanical/molecular mechanics calculations, with the ONIOM (B3PW91/UFF) method, have been carried out on the full

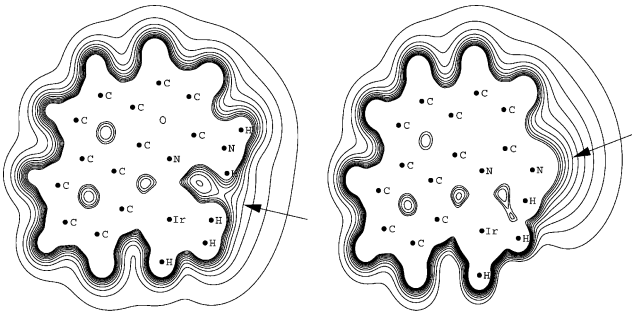

7 8

Fig. 4 Contour plot of the electrostatic potential in the plane of the bq ligand for **7** and **8**. Contour lines are shown from 0.1 a.u. to 0.3 a.u. in 0.02 increments.

systems $[IrH(H_2)(bq\text{-}NH_2)(PPh_3)_2][BF_4]$, **9**, and $[Ir(H)_2(bq\text{-}NH_3)(PPh_3)_2][BF_4]$, **10**. Only the phenyl groups of the PPh_3 ligands have been treated at the MM level, all the remaining atoms, and particularly the counter anion BF_4^-, were treated within the DFT framework.

For both systems, the position of the anion was in agreement with the analysis based on the electrostatic potential and the optimized geometries are shown in Fig. 5. BF_4^- is closer to the metal in **9** than in **10** (as illustrated by the Ir···B distances: 4.208 Å, **9**; 5.241 Å, **10**). In **9** there are two short H···F contacts between cation and anion, one with the H_2 ligand (H···F = 2.068 Å) and the other with the NH_2 group (H···F = 1.781Å). In **10**, three short contacts are present, but only with the NH_3^+ group (H···F = 1.668, 1.687, and 2.434 Å). As a consequence of the ion pair formation, the dihydrogen bond is longer in **10** than in **8** (H···H = 1.379 Å, **8**; H···H = 1.517 Å, **10**) and the N–H bond is shorter (N–H = 1.150 Å, **8**; N–H = 1.067 Å, **10**).

The inclusion of the counter anion reduces the relative energy between the two isomers with **9** (dihydrogen complex) now being only 3 kcal mol^{-1} more stable than **10** (hydride complex). When both components of the ONIOM energy are considered individually, the assumption of increased steric repulsion within **9** is confirmed. The energy difference between the QM parts of **9** *versus* **10** is 6 kcal mol^{-1} in favor of dihydrogen complex **9**, illustrating the stabilizing electronic contribution of ion pairing in **10**. This value should be compared with the 14.4 kcal mol^{-1} energy difference found between dihydrogen **7** and hydride **8**, implying that the anion stabilizes the hydride form by *ca.* 8 kcal mol^{-1}. For the MM parts, **9** is 3 kcal mol^{-1} *less* stable than **10**, confirming that ion pair formation close to the H_2 ligand introduces larger steric repulsions.

In our attempt to model ion pairing with NH_3^+ we expected to see H···F contacts with all the NH_3^+ protons as in **10**. However, the electrostatic potential for **8** (Fig. 4) reveals that ion pair formation is not restricted to the NH_3^+ group. In particular, H3 of bq is a viable candidate for such H···F short contacts. Indeed we optimized another minimum (Fig. 6), **11**, also with three short H···F contacts: two are with NH_3^+ (H···F = 1.652 and 1.661 Å) and one is with the H3 (H···F = 2.219 Å). The dihydrogen bond parameters in **11**

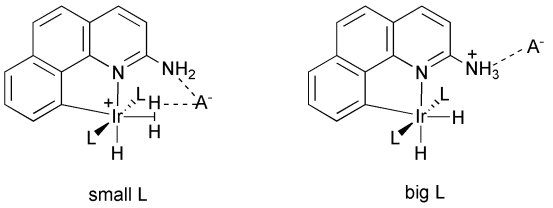

Scheme 2

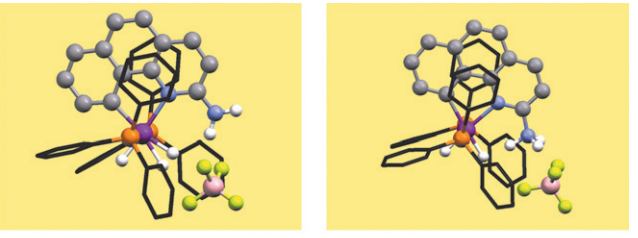

9 10

Fig. 5 Optimized geometry (ONIOM(B3PW91/UFF)) for the ion pair dihydrogen complex $[IrH(H_2)(bq\text{-}NH_2)(PPh_3)_2][BF_4]$, **9**, and the ion pair hydride complex $[Ir(H)_2(bq\text{-}NH_3)(PPh_3)_2][BF_4]$, **10**. Atoms included in the QM part are shown in ball-and-stick format and atoms included in the MM part are shown in black.

differ from those in **10** (H···H = 1.517 Å, N–H = 1.067 Å, **10**; H···H = 1.539 Å, N–H = 1.060 Å, **11**) as the N–H proton is not directly involved in the interaction with BF_4^-.

Complex **11** is marginally less stable than **9** but by only 0.4 kcal mol^{-1}; the QM parts differ by only 1.9 kcal mol^{-1} as a result of an optimal arrangement for anion–cation specific interactions in **11**.

In conclusion the ONIOM calculations strongly suggest that ion pairing is responsible for the unexpected experimental observation of **6** in the case of L = PPh_3. With close contacts between acidic protons and BF_4^-, strong electronic preference for the dihydrogen complex may be strongly reduced as illustrated by **9** and **11**. Electronic and steric components of the ion pairing energy contribute to the effect with a more efficient interaction and a weaker steric repulsion in the hydride isomers.

Experimental probes of ion pairing

Unfortunately, experimental attempts to exchange the BF_4^- counter-anion of **6a** and **6e** in a CD_2Cl_2 solution at −80 °C with a smaller one, like F^-, with the goal of switching the isomer to the unobserved dihydrogen complex **5a,e**, all failed. Instead, we always obtained the neutral dihydride $[Ir(bq\text{-}NH_2)(PR_3)_2)(H)_2]$ formed by deprotonation of the NH_3^+ group by F^-, acting as a base. Even using the weaker base, Cl^-, led to the same deprotonation. This deprotonation product was known because it had been already synthesized by another route, the action of $NaBH_4$ on the aqua or acetone complexes.

Polar solvents can separate tight ion pairs, but all attempts in our system led to displacement of the coordinated H_2 and formation of the solvent complex where the labile site is occupied by the solvent.

$^{19}F,^1H$-HOESY NMR spectra have previously[7] given invaluable information on ion pair structure by revealing contacts between the BF_4^- or PF_6^- anions and the complex

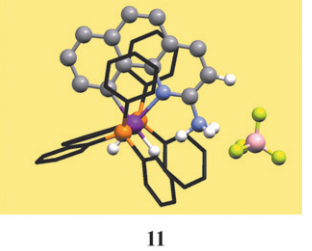

11

Fig. 6 Alternate ion pair geometry for the hydride complex $[Ir(H)_2(bq\text{-}NH_3)(PPh_3)_2][BF_4]$, **11**. The H3 proton bq is explicitly shown to illustrate the close contact with BF_4^-. Atoms included in the QM part are shown in ball-and-stick format and atoms included in the MM part are shown in black.

cation. Some of the hydride complexes **5** and **6** studied here proved unsuitable, however, because of thermal instability and solubility problems. Two related stable and soluble complexes, $[Ir(bq\text{-}H)(PPh_3)_2H(CO)]PF_6$,[18] and $[Ir(bq\text{-}NH_2)(PPh_3)_2H(CO)]PF_6$, did give good data. The anion–cation contacts observed in the NMR spectrum (CD_2Cl_2, 208 K, 376.63 MHz)[19] showed the anions in the expected locations, next to the bq-H 2- and 3-positions in the former and next to the amino group in the latter. Contacts with *ortho* and *meta* PPh_3 protons were also detected. For the key case of $[Ir(bq\text{-}NH_3)(PPh_3)_2(H)_2]PF_6$, **6a**, formed in equilibrium from **4′a** and H_2, data were obtained showing strong contacts for the bq-NH_3^+ proton, as predicted by the theoretical study. Contacts with the *ortho* and *meta* PPh_3 protons as well as the 3-protons of bq were seen but no contacts with the Ir–H protons. The theoretical prediction was therefore in excellent agreement with the subsequent experimental confirmation by NMR spectroscopy.

Conclusion

The equilibrium between the $M(H_2)(bq\text{-}NH_2)$ and $MH(bq\text{-}NH_3)$ isomers seems to be decided by ion pairing effects. Theoretical studies in which no anion is included show that the $M(H_2)(bq\text{-}NH_2)$ form is predicted to be more stable for all the phosphines used. The observation of the $MH(bq\text{-}NH_3)$ isomer for bulky phosphines is therefore anomalous. The calculated electrostatic potentials for the two isomers suggest that the counter anion should be paired much closer to the metal in the $M(H_2)(bq\text{-}NH_2)$ case but that in the $MH(bq\text{-}NH_3)$ isomer it can be much farther from the metal. Bulky phosphines seem to favor remote ion pairing and therefore the $MH(bq\text{-}NH_3)$ isomer where steric effects disfavor close ion pairing.

Experimental section

All operations were carried out under argon atmosphere using standard Schlenk techniques. Solvents were dried over calcium hydride (CH_2Cl_2) or sodium/benzophenone (Et_2O). Solvents were degassed prior use. IR spectra were recorded on a Midac M1200 FT-IR spectrometer. Microanalyses were carried out by Robertson Microlit Laboratories. ^1H NMR and $^{31}P\{^1H\}$ NMR spectra were either recorded on GE Omega 300 or GE Omega 500 spectrometers, chemical shifts were measured with reference to the residual solvent resonance. The starting $[Ir(cod)L_2]X$ (X = BF_4 or PF_6) complexes were made as previously reported.[11a,b]

(2-Amino-7,8-benzoquinolinato)(solvento)bis(tri(*p*-tolyl)phosphine)iridium(III) salts (4, solvent = water; 4′ solvent = acetone)

These compounds can be prepared by one of three related methods. In **method A** (for **4**), reported previously,[10] $[Ir(cod)L_2]X$ (X = BF_4 or PF_6; 0.25 mmol) and 2-aminobenzoquinoline (0.25 mmol) in CH_2Cl_2 (10 ml) are treated with H_2 (1 atm) for 30 min at 0 °C (ice bath). The solvent volume is reduced by 50% on the vacuum line and the product is precipitated with hexanes–Et_2O (1:1, 10 ml) and recrystallized from CH_2Cl_2/Et_2O. **Method B** (for **4′**) goes through an intermediate acetone complex $[IrH_2(Me_2CO)_2L_2]X$.[20] $[Ir(cod)L_2]X$ (0.25 mmol) in acetone (10 ml) is first treated with H_2 (1 atm) for 30 min at 0 °C (ice bath). The intermediate is then precipitated with Et_2O then redissolved in acetone (10 ml) to which is added 2-aminobenzoquinoline (0.25 mmol) in acetone (10 ml). The mixture is stirred for 30 min and the final product precipitated with hexanes and recrystallized from CH_2Cl_2/Et_2O. **Method C** (for **4**), goes through an intermediate aqua complex $[IrH_2(H_2O)_2L_2]X$.[20] $[Ir(cod)L_2]X$ (0.25 mmol) in moist CH_2Cl_2 (10 ml) is first treated with H_2 (1 atm) for 30 min at 0 °C (ice bath). The intermediate is then precipitated with hexanes and redissolved in moist CH_2Cl_2 (10 ml). Aminobenzoquinoline (0.25 mmol) is then added and the mixture stirred for 30 min. The final product is precipitated with hexanes and recrystallized from CH_2Cl_2/Et_2O.

4a (BF_4 salt). The complex was previously prepared by method A.[10]

4b (PF_6 salt). The complex was best prepared by method C. ^1H NMR (CD_2Cl_2, 500 MHz, 293K, ppm) δ −16.61 (br. s, Ir–H), 1.60 (br. s, 2H, H_2O), 2.22 (s, 18H, Me), 6.00–8.10 (m, 39H, bq + NH_2 + Ph). ^1H NMR (CD_2Cl_2, 500 MHz, 183 K, ppm) δ −16.61 (br. s, Ir–H), 1.60 (br. s, 2H, H_2O), 2.22 (s, 18H, Me), 6.00–8.10 (m, 39H, bq + NH_2 + Ph). $^{31}P\{^1H\}$ NMR (CD_2Cl_2, 125 MHz, 293 K, ppm) δ 18.83 (s). IR (thin film, cm^{-1}): ν 2186.7 (IrH), 3361.1 (NH), 3464.2 (NH). Anal. Calcd. for $C_{55}H_{54}F_6IrN_2OP_3$: C, 57.04, H, 4.70, N, 2.42%. Found: C, 56.89, H, 4.66, N, 2.28%. Yield: 80%.

4c (PF_6 salt). The complex was best prepared by method C. ^1H NMR (CD_2Cl_2, 500 MHz, 293 K, ppm) δ −16.76 (br. s, 1H, Ir–H), 1.89 (br. s, 2H, H_2O), 3.72 (s, 18H, OMe), 6.20–8.00 (m, 33H, bq + NH_2 + Ph). ^1H NMR (CD_2Cl_2, 500 MHz, 183 K, ppm) δ −16.61 (br. s, Ir–H), 1.60 (br. s, 2H, H_2O), 2.22 (s, 18H, Me), 6.00–8.10 (m, 39H, bq + NH_2 + Ph). $^{31}P\{^1H\}$ NMR (CD_2Cl_2, 125 MHz, 293 K, ppm) δ 16.69 (s). IR (thin film, cm^{-1}): ν 2212.3 (IrH), 3361.1 (NH), 3469.2 (NH). Anal. Calcd. for $C_{55}H_{54}F_6IrN_2O_7P_3$: C, 52.57, H, 4.34, N, 2.23%. Found: C, 52.48, H, 4.22, N, 2.25%. Yield: 81%.

4d (BF_4 salt). The complex was best prepared by method C. ^1H NMR (CD_2Cl_2, 500 MHz, 293 K, ppm) δ −16.77 (t, 1H, $^2J_{H-P}$ = 14.65 Hz, Ir–H), 1.50 (br. s, 2H, H_2O), 1.60 (s, 6H, Me), 6.24 (br. s, 2H, NH_2), 6.41–7.63 (m, 27H, bq + Ph). ^1H NMR (CD_2Cl_2, 500 MHz, 183 K, ppm) δ −16.34 (t, 1H, $^2J_{H-P}$ = 14.65 Hz, Ir–H), 1.70 (s, 2H, Me), 6.10 (s, 1H, NH_a) 6.39–7.89 (m, 28H, bq + NH_b + Ph). $^{31}P\{^1H\}$ NMR (CD_2Cl_2, 125 MHz, 293 K, ppm) δ 5.08 (s). IR (thin film, cm^{-1}): ν 2186.7 (IrH), 3319.8 (NH), 3412.7 (NH). Anal. Calcd. for $C_{39}H_{38}F_4IrN_2OP_2B$: C, 52.53, H, 4.29, N, 3.14%. Found: C, 52.42, H, 4.19, N, 2.94%. Yield: 42%.

(2-Amino-7,8-benzoquinolinato)(acetone)bis(tricyclohexylphosphine)iridium(III) hexafluorophosphate (4′e)

The complex was best prepared by a variant of method B. $[IrH_5(PCy_3)_2]$ (0.25 mmol) was dissolved in acetone (10 ml) to which 1.5 equiv. HPF_6 was added. The pale yellow intermediate, $[IrH_2(OCMe_2)_2(PCy_3)_2]PF_6$, was precipitated with Et_2O, dried *in vacuo* (240 mg, 0.22 mmol) and immediately carried forward by redissolving in acetone (10 ml). Addition of 2-amino-7,8-benzoquinoline (43.6 mg, 0.22 mmol) in acetone (10 ml) is carried out with stirring, followed by precipitation of the product after 15 min with hexane (100 ml). Recryst: CH_2Cl_2/Et_2O. ^1H NMR (CD_2Cl_2, 500 MHz, 293 K, ppm) δ −14.34 (t, 1H, $^2J_{H-P}$ = 14.65 Hz, Ir–H), 0.60–2.00 (m, 72H, Cy + CH_3COCH_3), 5.83 (s, 2H, NH_2), 6.55–8.30 (m, 7H, bq). ^1H NMR (CD_2Cl_2, 500 MHz, 183 K, ppm) δ −14.23 (t, 1H, $^2J_{H-P}$ = 14.65 Hz, Ir–H), 0.60–2.00 (m, 72H, Cy + CH_3COCH_3), 6.05 (s, 1H, NH_a) 6.70–8.50 (m, 7H, bq), 7.55 (s, 1H, NH_b). $^{31}P\{^1H\}$ NMR (CD_2Cl_2, 125 MHz, 293 K, ppm) δ 14.86 (s). IR (thin film, cm^{-1}): ν 1564 (C=O), 2176 (IrH), 3364 (NH), 3427 (NH). Anal. Calcd. for $C_{58}H_{58}F_6IrN_2O_7P_3$: C, 53.83, H, 4.52, N, 2.16%. Found: C, 53.60, H, 4.43, N, 2.27%. Yield: 82%.

Observation of reaction with H_2

The appropriate salt, **4**, (10 μmol) was dissolved in CD_2Cl_2 (0.5 ml) in an NMR tube with anhydrous $MgSO_4$ (5 mg) also present, cooled to −70 °C (EtOH bath cooled with liq. N_2) and H_2 passed for 30 min. The NMR tube was transferred to a pre-cooled probe (−80 °C) and the spectrum observed.

Spectrum of 6a. ^{1}H NMR (CD_2Cl_2, 500 MHz, 203 K, ppm) δ −25.63 (dt, 1H, $^2J_{H-H'}$ = 8.50 Hz, $^2J_{H-P}$ = 14.65 Hz, Ir–H), −23.24 (dt, 1H, $^2J_{H-H'}$ = 8.50 Hz, $^2J_{H-P}$ = 14.65 Hz, Ir–H), 4.56 (br. s, 3H, NH_3^+), 6.80–8.00 (m, 37H, bq + Ph). ^{1}H NMR (CD_2Cl_2, 500 MHz, 293 K, ppm) δ −25.83 (dt, 1H, $^2J_{H-H'}$ = 8.50 Hz, $^2J_{H-P}$ = 14.65 Hz, Ir–H), −23.19 (dt, 1H, $^2J_{H-H'}$ = 8.50 Hz, $^2J_{H-P}$ = 14.65 Hz, Ir–H), 1.70 (br. s, 2H, free H_2O), 4.69 (br. s, 3H, NH_3^+), 6.80–8.00 (m, 37H, bq + Ph).

6b. ^{1}H NMR (CD_2Cl_2, 500 MHz, 203 K, ppm) δ −25.91 (br. s, 1H, Ir–H), −23.38 (br. s, 1H, Ir–H), 2.14 (s, 3H, Me), 4.15 (br. s, 3H, NH_3^+), 6.56–8.14 (m, 31H, bq + Ph).

6c. ^{1}H NMR (CD_2Cl_2, 500 MHz, 203 K, ppm) δ −26.10 (br. s, 1H, Ir–H), −23.44 (br. s, 1H, Ir–H), 3.66 (s, 3H, OMe), 4.29 (br. s, 3H, NH_3^+), 6.42–8.24 (m, 31H, bq + Ph).

6e. ^{1}H NMR (CD_2Cl_2, 500 MHz, 203 K, ppm) δ −25.03 (br. s, 1H, Ir–H), −21.06 (br. s, 1H, Ir–H), 0.60–2.40 (m, 60H, Cy), 4.29 (br. s, 3H, NH_3^+), 6.28–8.62 (m, 7H, bq).

5d. ^{1}H NMR (CD_2Cl_2, 500 MHz, 208 K, ppm) δ −15.90 (br. s, 1H, Ir–H), −3.75 (br. s, 2H, Ir–H_2), 1.70 (s, Me), 5.52 (s, NH_2) 6.3–7.8 (m, bq + Ph).

(2-Amino-7,8-benzoquinolinato)(carbonyl)bis(tricyclohexylphosphine)iridium(III) hexafluorophosphate

For the case of the benzoquinolinate with L = PPh_3, the complex has been reported and structurally characterized.[17] For the present complexes, the same method, treating **4** or **4′** (0.15 mmol) in CH_2Cl_2 (10 ml) with CO (1 atm) for 30 min, isolating with hexanes, then recrystallizing from CH_2Cl_2/hexanes, was used.

L = PPh_3. ^{1}H NMR (CD_2Cl_2, 500 MHz, 293 K, ppm) δ −14.98 (t, 1H, $^2J_{HP}$ = 12.21 Hz, Ir–H), 5.66 (s, 2H, NH_2), 6.87–7.60 (m, 37H, bq + Ph). ^{31}P{^{1}H} NMR (CD_2Cl_2, 125 MHz, 293 K, ppm) δ 7.16 (s). IR (thin film, cm^{-1}): ν 2026.0 (C=O), 2222.6 (Ir–H), 3397.1 (N–H), 3510.5 (N–H). Anal. Calcd. for $C_{50}H_{40}F_6IrN_2OP_3$: C, 55.40, H, 3.72, N, 2.58%. Found: C, 55.07, H, 3.72, N, 2.48%. Yield: 83%. Yellow solid.

L = $P(p\text{-}C_6H_4CH_3)_3$. ^{1}H NMR (CD_2Cl_2, 500 MHz, 293 K, ppm) δ −15.07 (t, 1H, $^2J_{HP}$ = 12.21 Hz, Ir–H), 2.24 (s, 18H, Me), 5.61 (s, 2H, NH_2), 6.87–7.62 (m, 31H, bq + Ph). ^{31}P{^{1}H} NMR (CD_2Cl_2, 125 MHz, 293 K, ppm) δ 5.36 (s). IR (thin film, cm^{-1}): ν 2024.5 (C=O), 2227.7 (Ir–H), 3392.0 (N–H), 3510.5 (N–H). Anal. Calcd. for $C_{56}H_{52}F_6IrN_2OP_3$–CH_2Cl_2: C, 54.63, H, 4.34, N, 2.23%. Found: C, 54.94, H, 4.39, N, 2.09%. Yield: 83%. Pale pink solid.

L = $P(p\text{-}C_6H_4OCH_3)_3$. ^{1}H NMR ($CD_2Cl_2$, 500 MHz, 293 K, ppm) δ −15.14 (t, 1H, $^2J_{HP}$ = 12.21 Hz, Ir–H), 3.74 (s, 18H, OMe), 5.79 (s, 2H, NH_2), 6.57–7.66 (m, 31H, bq + Ph). ^{31}P{^{1}H} NMR (CD_2Cl_2, 125 MHz, 293 K, ppm) δ 2.85 (s). IR (thin film, cm^{-1}): ν 2023.4 (C=O), 2226.9 (Ir–H), 3397.4 (N–H), 3505.8 (N–H). Anal. Calcd. for $C_{56}H_{52}F_6IrN_2O_7P_3$–$CH_2Cl_2$: C, 50.75, H, 4.03, N, 2.08%. Found: C, 50.31, H, 4.09, N, 1.81%. Yield: 82%. Pale pink solid.

L = $PMePh_2$. ^{1}H NMR (CD_2Cl_2, 500 MHz, 293 K, ppm) δ −15.52 (t, 1H, $^2J_{HP}$ = 12.48 Hz, Ir–H), 1.72 (s, 6H, Me), 5.96 (s, 2H, NH_2), 6.80–8.84 (m, 27H, bq + Ph). IR (thin film, cm^{-1}): ν 2021.7 (C=O), 2197.0 (Ir–H), 3391.9 (N–H), 3479.5 (N–H). Not obtained analytically pure.

L = PCy_3. ^{1}H NMR (CD_2Cl_2, 500 MHz, 293 K, ppm) δ −16.63 (t, ^{1}H, $^2J_{HP}$ = 14.65 Hz, Ir–H), 1.00–2.00 (m, 60H, Cy), 6.06 (s, 2H, NH_2), 7.0–8.3 (m, 7H, bq). ^{31}P{^{1}H} NMR (CD_2Cl_2, 125 MHz, 293 K, ppm) δ 2.26 (s). IR (thin film, cm^{-1}): ν 1994.5 (C=O), 2121.5 (Ir–H), 3353.0 (N–H), 3508.2 (N–H). Not obtained analytically pure.

Improved synthesis of pentahydridobis(tricyclohexylphosphine)-iridium(V)

Hydrogen gas was bubbled overnight at room temperature in an orange suspension of $[Ir(cod)Cl]_2$ (1 eq, 685 mg, 0.98 mmol), PCy_3 (4 eq, 1100 mg, 3.92 mmol) and NaOMe (2 eq, 106 mg, 1.96 mmol) in degassed dichloromethane (40 mL), under stirring. A white solid was obtained by filtration *in vacuo*, washed with H_2O, then Et_2O, and dried *in vacuo* (877 mg, 59%). ^{1}H NMR (CD_2Cl_2, 500 MHz, 293 K, ppm) δ −11.27 (t, 5H, $^2J_{HP}$ = 12.21 Hz, Ir–H), 1.10–2.25 (m, 66H, Cy). ^{31}P{^{1}H} NMR (CD_2Cl_2, 125 MHz, 293 K, ppm) δ 33.42 (s). IR (thin film, cm^{-1}): ν(Ir–H) 1929.1. Anal. Calcd. for $C_{36}H_{68}IrP_2Cl.0.33CH_2Cl_2$: C, 55.51, H, 9.19%. Found: C, 55.65, H, 8.69%. Yield: 59%.

^{19}F,^{1}H-HOESY NMR spectra

These were obtained following the procedure of ref. 17.

Computational details

All calculations were performed with the Gaussian 98 set of programs[21] within the framework of hybrid DFT (B3PW91)[22] for complexes **7** and **8** and with the ONIOM method[23] for complexes **9**, **10**, and **11**. These three complexes were optimized at the ONIOM(B3PW91/UFF) level, where the QM part was treated within the framework of density functional theory at the B3PW91 level[22] and the UFF force field[24] was used for the molecular mechanics calculations. In all calculations (QM and QM/MM) the iridium atom was represented by the relativistic effective core potential (RECP) from the Stuttgart group (17 valence electrons) and its associated (8s7p5d)/[6s5p3d] basis set,[25] augmented by an f polarization function (α = 0.95). The phosphorus atoms were also treated with Stuttgart's RECPs and the associated basis set,[26] augmented by a polarization d function (α = 0.387). A 6-31G(d,p) basis set was used for the atoms directly bound to Ir (N,C, and H) and the atoms of the NH_2 (or NH_3) group. The remaining atoms were treated by a 6-31G basis set. Full optimizations of geometry without any constraint were performed for both types of calculations (B3PW91 and ONIOM(B3PW91/UFF)), followed by analytical computation of the Hessian matrix to confirm the nature of the located extrema as minima on the potential energy surface. ΔG values were calculated at 298 K within the harmonic frequency approximation.

Acknowledgements

This work was supported by grants from the Ministero dell'Universitá e della Ricerca Scientifica e Tecnologica (MURST, Rome, Italy), Programma di Rilevante Interesse Nazionale, Cofinanziamento 2000-1 (A. M.), the CNRS and the Université Montpellier II (E. C. and O. E.), and the DOE (R. H. C., K. G.). R. H. C. thanks the Université Montpellier II for a position of invited professor.

References

1 P. J. Brothers, *Prog. Inorg. Chem.*, 1981, **28**, 1.
2 D. M. Heinekey and W. J. Oldham Jr, *Chem. Rev.*, 1993, **93**, 913.
3 Y. Nicolet, A. Y. de Lacey, X. Vernede, V. M. Fernandez, E. C. Hatchikian and J. C. Fontecilla-Camps, *J. Am. Chem. Soc.*, 2001, **123**, 1596.
4 D.-H. Lee, B. Patel, E. Clot, O. Eisenstein and R. H. Crabtree, *Chem Commun.*, 1999, 297.
5 R. H. Morris, *Can. J. Chem.*, 1996, **74**, 1907.
6 J. A. Ayllon, S. F. Sayers, S. Sabo-Etienne, B. Donnadieu, B. Chaudret and E. Clot, *Organometallics*, 1999, **18**, 3981.
7 (*a*) C. Zuccaccia, G. Bellachioma, G. Cardaci and A. Macchioni, *J. Am. Chem. Soc.*, 2001, **123**, 11 020 and refs. cited; (*b*) G. Lanza, I. L. Fragala and T. J. Marks, *J. Am. Chem. Soc.*, 2000, **122**, 12 764
8 R. H. Crabtree, M. Lavin and L. Bonneviot, *J. Am. Chem. Soc.*, 1986, **108**, 4032.
9 H. Vorbrüggen, *Adv. Heterocycl. Chem.*, 1990, **49**, 117.
10 (*a*) B. Patel, D.-H. Lee, A. L. Rheingold and R. H. Crabtree, *Organometallics*, 1999, **18**, 1615; (*b*) K. Gruet, R. H. Crabtree, D.-H. Lee, L. Liable-Sands and A. L. Rheinold, *Organometallics*, 2000, **19**, 2228.
11 (*a*) R. H. Crabtree and G. E. Morris, *J. Organomet. Chem.*, 1977, **135**, 395; (*b*) R. H. Crabtree, H. Felkin and G. E. Morris, *J. Organomet. Chem.*, 1977, **141**, 205; (*c*) S. Brinkmann, R. H. Morris, R. Ramachandran and S.-H. Park, *Inorg. Synth.*, 1998, **32**, 303.
12 A. Tolman, *Chem Rev.*, 1977, **77**, 313.
13 see Computational Details.
14 R. H. Crabtree, P. E. M. Siegbahn, O. Eisenstein, A. L. Rheingold and T. F. Koetzle, *Acc. Chem. Res.*, 1996, **29**, 348.
15 L. Perrin, E. Clot, O. Eisenstein, J. Loch and R. H. Crabtree, *Inorg. Chem.*, 2001, **40**, 5806.
16 K. Miyabe, S. Taguchi, I. Kasahara and K. J. Goto, *J. Phys. Chem. B*, 2000, **104**, 8481 and refs cited.
17 A. Macchioni, C. Zuccaccia, E. Clot, K. Gruet and R. H. Crabtree, *Organometallics*, 2001, **20**, 2367.
18 (*a*) F. Neve, M. Ghedini, A. Tiripicchio and F. Ugozzoli, *Inorg. Chem.*, 1989, **28**, 3084; (*b*) T. Dubé, J. W. Faller and R. H. Crabtree, *Inorg. Chem.*, 2002, **41**, 5561.
19 A potentially relevant issue in this chemistry is that the ε of the solvent is known to increase very greatly with decreasing temperature over the range used here, going from 9 at 298 K to 16 at 208 K.[27] This is expected to counteract somewhat the normal entropy-based tendency for increasing ion pairing at low temperature.
20 R. H. Crabtree, P. C. Demou, D. Eden, J. M. Mihelcic, C. Parnell, J. M. Quirk and G. E. Morris, *J. Am. Chem. Soc.*, 1982, **104**, 6994.
21 M. J. Frisch, G. W. Trucks, H. B. Schlegel, G. E. Scuseria, M. A. Robb, J. R. Cheeseman, V. G. Zakrzewski, J. A. Montgomery, R. E. Stratmann, J. C. Burant, S. Dapprich, J. M. Millam, A. D. Daniels, K. N. Kudin, M. C. Strain, O. Farkas, J. Tomasi, V. Barone, M. Cossi, R. Cammi, B. Mennucci, C. Pomelli, C. Adamo, S. Clifford, J. Ochterski, G. A. Petersson, P. Y. Ayala, Q. Cui, K. Morokuma, D. K. Malick, A. D. Rabuck, K. Raghavachari, J. B. Foresman, J. Cioslowski, J. V. Ortiz, B. B. Stefanov, G. Liu, A. Liashenko, P. Piskorz, P. I. Komaromi, G. Gomperts, R. L. Martin, D. J. Fox, T. Keith, M. A. Al-Laham, C. Y. Peng, A. Nanayakkara, C. Gonzalez, M. Challacombe, P. M. W. Gill, B. G. Johnson, W. Chen, M. W. Wong, J. L. Andres, M. Head-Gordon, E. S. Replogle and J. A. Pople, Gaussian 98 (Rev A7), Gaussian, Inc., Pittsburgh, PA, 1998.
22 (*a*) A. D. J. Becke, *J. Chem. Phys.*, 1993, **98**, 5648; (*b*) J. P. Perdew and Y. Wang, *Phys. Rev. B*, 1992, **82**, 284.
23 M. Svensson, S. Humbel, R. D. J. Froese, T. Matsubara, S. Sieber and K. J. Morokuma, *J. Phys. Chem.*, 1996, **100**, 19 357.
24 A. K. Rappé, C. J. Casewitt, K. S. Colwell, W. A. Goddard and W. M. Skiff, *J. Am. Chem. Soc.*, 1992, **114**, 10 024.
25 D. Andrae, U. Häussermann, M. Dolg, H. Stoll and H. Preuss, *Theor. Chim. Acta*, 1990, **77**, 123.
26 A. Bergner, M. Dolg, W. Küchle, H. Stoll and H. Preuss, *Mol. Phys.*, 1990, **30**, 1431.
27 S. O. Morgan and H. H. Lowry, *J. Phys. Chem.*, 1930, **34**, 2385.